

Point Defect-Driven Switching of Conductivity Type in Bi_2Te_3 Films

Prepared by Atomic Layer Deposited

Tao Guo^a, Shuo Li^b, Xu Li^b, Guiying Xu^{a*}, Bohang Nan^a, Lingling Ren^b

^a School of Materials Science and Engineering, University of Science and Technology Beijing, Beijing 100083, China;

^b Center for Advanced Measurement Science, National Institute of Metrology, Beijing 100029, China;

* Corresponding author: guiyngxu@126.com

1. The microtopography of substrate and samples.

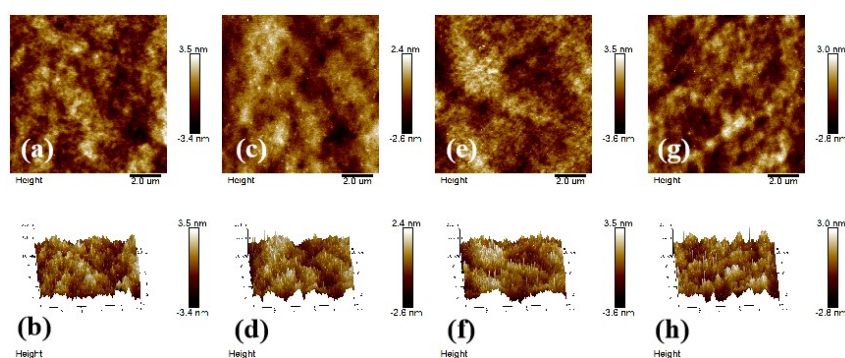


Fig. S1 The AFM morphologies of cleansed substrate (a, b) No.1, (c,d) No.2, (e,f) No.3 and (g,h) No.4.

1.1 The influence of $(\text{Et}_3\text{Si})_2\text{Te}$ temperature

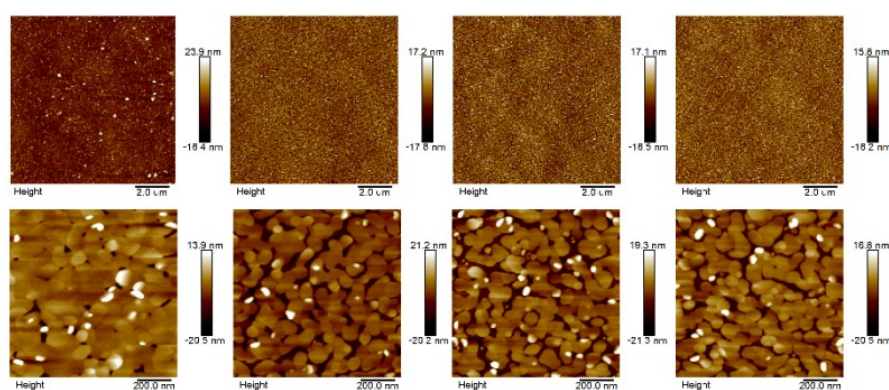


Fig. S2 The AFM morphologies on substrate (a, b) No.1, (c,d) No.2, (e,f) No.3, (g,h) No.4 at $(\text{Et}_3\text{Si})_2\text{Te}$ temperatures of 50°C.

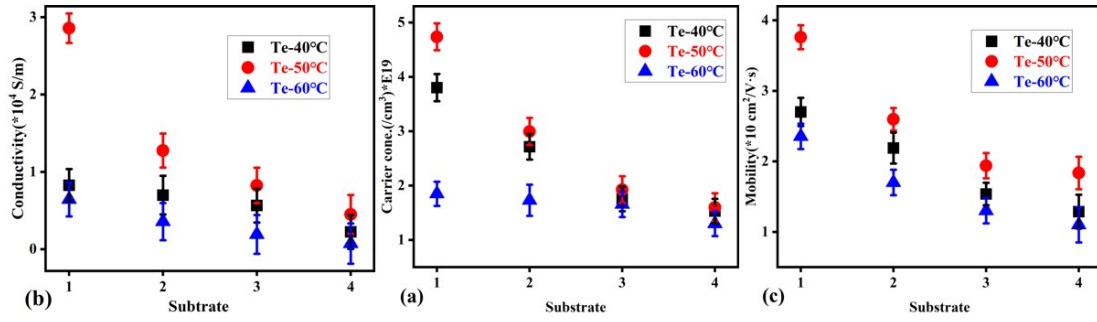


Fig. S3 The (a) carrier concentration, (b) electrical conductivity, and (c) mobility corresponding to temperature-index of $(\text{Et}_3\text{Si})_2\text{Te}$ under different substrate.

1.2 The influence of deposition temperature

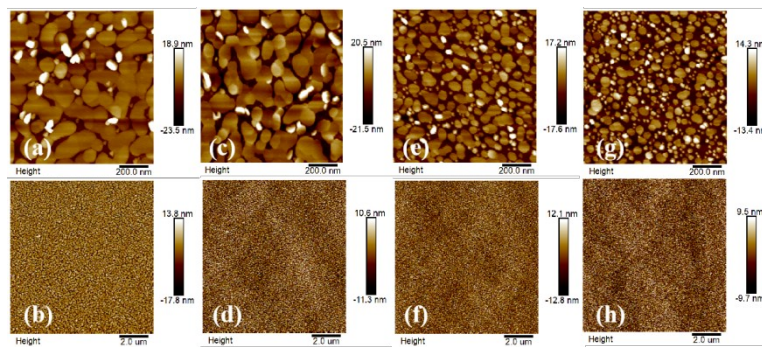


Fig. S4 The AFM morphologies on substrate (a, b) No.1, (c, d) No.2, (e, f) No.3, (g, h) No.4 at deposition temperatures of 200°C.

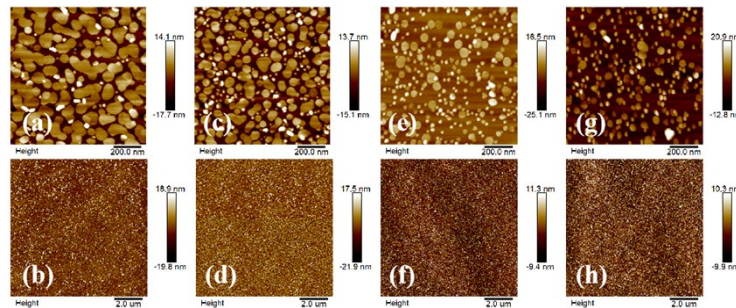


Fig. S5 The AFM morphologies on substrate (a, b) No.1, (c, d) No.2, (e, f) No.3, (g, h) No.4 at deposition temperatures of 210°C.

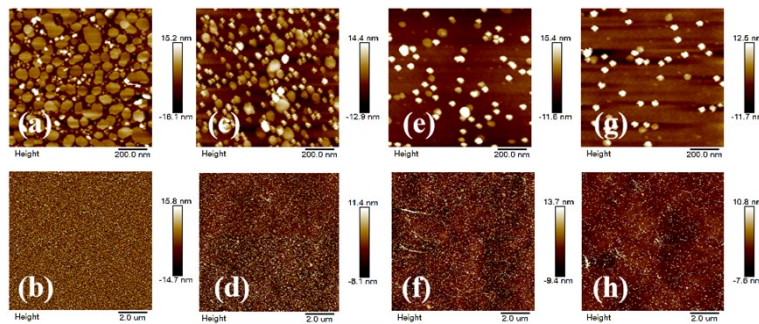


Fig. S6 The AFM morphologies on substrate (a, b) No.1, (c, d) No.2, (e, f) No.3, (g, h) No.4 at deposition temperatures of 220°C.

1.3 The influence of Cycle-Index (Thickness)

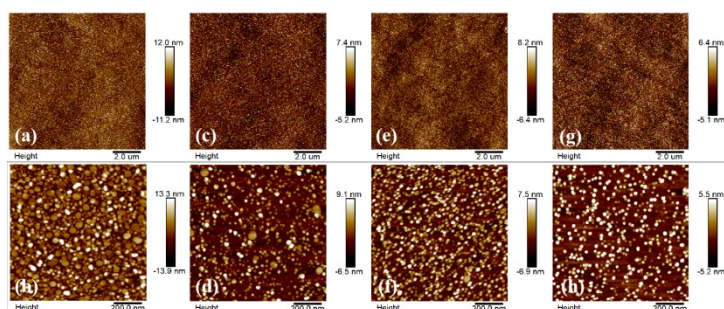


Fig. S7 The AFM morphologies on substrate (a, b) No.1, (c,d) No.2, (e,f) No.3, (g,h) No.4 at 50 cycle

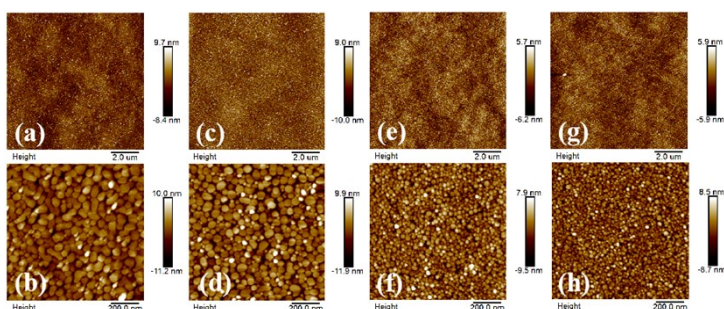


Fig. S8 The AFM Morphologies on substrate (a, b) NO.1, (c,d) NO.2, (e,f) NO.3, (g,h) NO.4 at 100 cycle

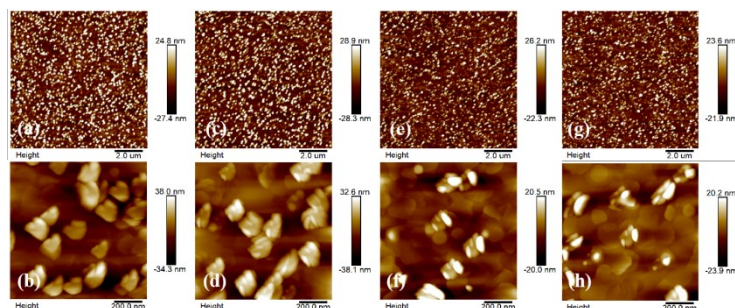


Fig. S9 The AFM morphologies on substrate (a, b) No.1, (c,d) No.2, (e,f) No.3, (g,h) No.4 at 400 cycle

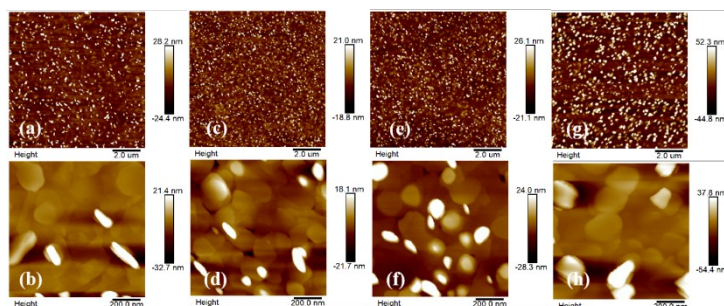


Fig. S10 The AFM morphologies on substrate (a, b) No.1, (c,d) No.2, (e,f) No.3, (g,h) No.4 at 600 cycle

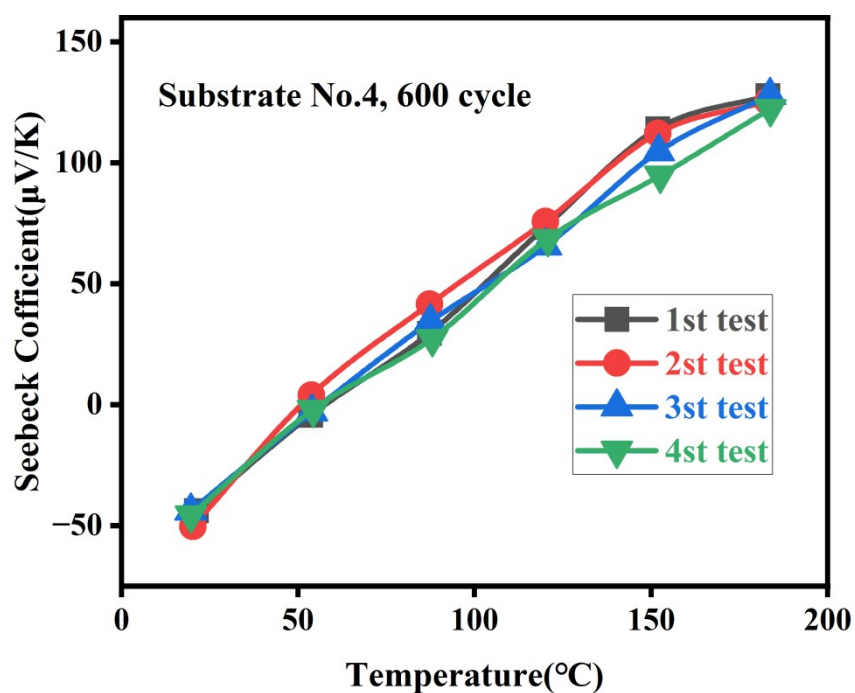


Fig.S11 Raw data showing the Seebeck coefficient as a function of temperature for a representative sample.

2. The SEM images of samples under 600 cycles.

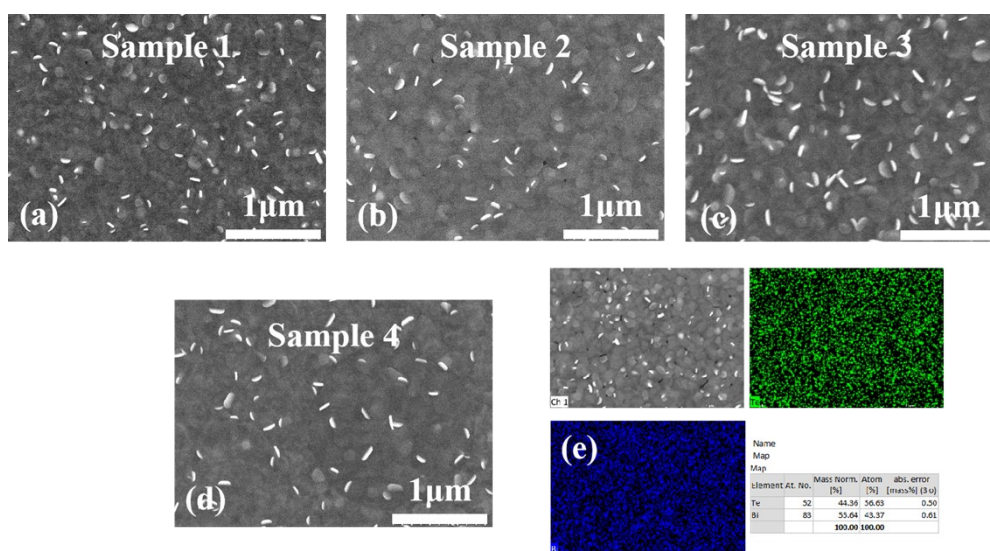


Fig.S12 The corresponding SEM images of samples from(a-d) 1 to 4 and EDS (e) of sample 1 under 600 cycles.

It can be seen from Fig.S12 results that the films prepared by this condition possess excellent coverage and crystallinity, with EDS confirming uniform element distribution. Te volatility leads to a deficiency in the sample, which exhibits n-type conductivity.

Table S1 The EDS analysis of all continuous film samples

Substrate	400 cycle		600 cycle	
	Te	Bi	Te	Bi
No.1	58.88	41.12	56.63	43.37
No.2	58.42	41.58	56.25	43.75
No.3	57.96	42.04	55.98	44.02
No.4	57.65	42.35	55.63	44.37

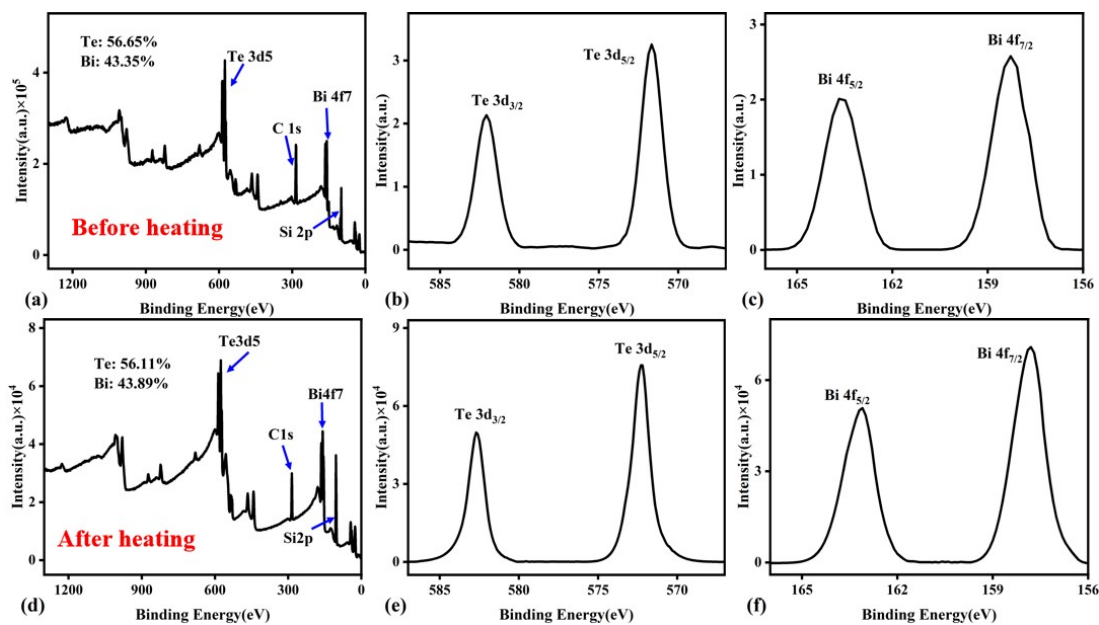


Fig.S13 The corresponding SEM images of samples from(a-d) 1 to 4 and EDS (e) of sample 1 under 600 cycles.